

## A Spectroscopic Study on the Interaction between Ferric Oxide Nanoparticles and Human Hemoglobin

S. Zolghadri, A.A. Saboury\*, E. Amin and A.A. Moosavi-Movahedi  
*Institute of Biochemistry and Biophysics, University of Tehran, Tehran, Iran*

*(Received 1 September 2009, Accepted 5 March 2010)*

Magnetic nanoparticles can promote many attractive functions in biomedicine, which may contribute to the prevention of human disease but also may be potentially harmful. In the present study, the interaction of Fe<sub>2</sub>O<sub>3</sub> nanoparticles with human hemoglobin (Hb) was studied by fluorescence, circular dichroism and UV/vis spectroscopies. Fluorescence data revealed that the fluorescence quenching of Hb by Fe<sub>2</sub>O<sub>3</sub> nanoparticles was the result of the formed complex of Fe<sub>2</sub>O<sub>3</sub> nanoparticles–Hb. Binding constants and other thermodynamic parameters were determined at three different temperatures. The hydrophobic interactions are the predominant intermolecular forces to stabilize the complex. Circular dichroism studies did not show any changes in the content of secondary structure of hemoglobin after Fe<sub>2</sub>O<sub>3</sub> nanoparticles treatment. This study provides important insight into the interaction of Fe<sub>2</sub>O<sub>3</sub> nanoparticles with hemoglobin, which may be a useful guideline for further using of these nanoparticles in biomedical applications.

**Keywords:** Fe<sub>2</sub>O<sub>3</sub> Nanoparticle, Human hemoglobin (Hb), Circular dichroism, Fluorescence

---

### INTRODUCTION

In the last decade, nanotechnology has developed to such an extent that it has become possible to fabricate, characterize and specially tailor the functional properties of nanoparticles for biomedical applications and diagnostics [1-4]. In this field, nanoparticles of magnetic metals and oxides have attracted great interest in recent years because of their unique physical and chemical properties [5]. Due to their suitable surface chemistry, ferric oxide magnetic (Fe<sub>2</sub>O<sub>3</sub>) nanoparticles offer a great of interest for biomedical applications, such as drug delivery, cell engineering, magnetic carriers for bioseparation and for enzyme and protein immobilization, tissue repair, diagnostics, and as a contrast-enhancing medium [6-11]. Ferromagnetic particles have also been used for various

in vivo applications such as a tracer of blood flow, in radionuclide angiography, and for use in inducing clotting in arteriovenous malformations [12]. Recently, magnetic nanoparticles have been used in magnetic resonance (NMR/MRI) techniques to detect molecular interactions [13]. For application in biological organisms, these particles have to be biocompatible. When nanoparticles of Fe<sub>2</sub>O<sub>3</sub> are injected into the blood for drug delivery and MRI imaging, the interaction of these particles with blood proteins must be decreased by suitable surface coating. However, these nanoparticles may interact with proteins and these interactions alter the structure and function of proteins. Hemoglobin is the major hemoproteins of red blood cell (RBC), which can reversibly bind with many kinds of endogenous and exogenous agents [14]. However, there are a few reports on the interaction of magnetic nanoparticles with hemoglobin (Hb).

---

\*Corresponding author. E-mail: saboury@ut.ac.ir

Hb is a tetramer composed of 4 globin molecules; 2 alpha globins and 2 beta globins. The alpha globin chain is composed of 141 amino acids and the beta globin chain is composed of 146 amino acids [15]; each globin chain also contains one heme molecule. The heme molecule is composed of a porphyrin ring and an iron ion ligand bound in the center [16]. Hb is well known for its function in the vascular system of animals, being a carrier of oxygen. There are four oxygen-binding sites on the Hb molecule. The main function of hemoglobin is to transport oxygen from the lungs to the tissues and then transport CO<sub>2</sub> back from the tissues to the lungs. The oxygen affinity of hemoglobin can also be regulated by external chemical factors including pH, carbon dioxide, and DPG (2,3-diphosphoglycerate). In this paper, we will address the binding of Fe<sub>2</sub>O<sub>3</sub> nanoparticle to Hb and the effect of Fe<sub>2</sub>O<sub>3</sub> nanoparticle on the protein structure is investigated by UV-Visible, fluorescence and circular dichroism (CD) spectroscopic techniques. The thermodynamic aspects in the binding process will be studied.

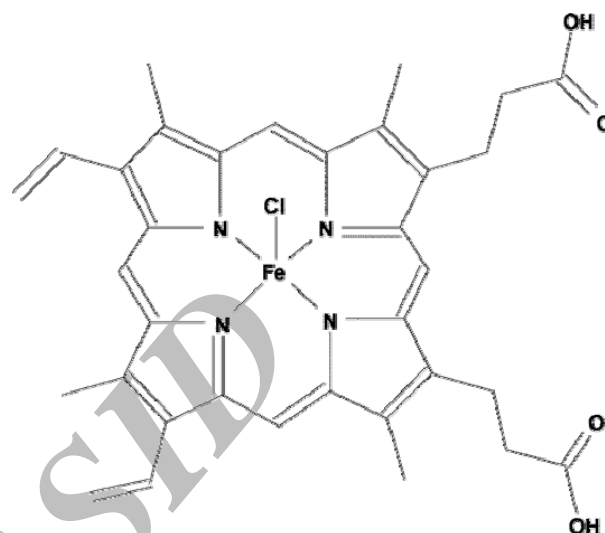
## EXPERIMENTAL

### Materials

Human Hb and Hemin (ferriprotoporphyrin IX chloride, scheme 1) was purchased from Sigma. Fe<sub>2</sub>O<sub>3</sub> nanoparticle was gifted from the Department of chemistry, University of Tehran (10-20 nm, liquid form, dispersion matrix: ethylenglycole, pH=7-8) Phosphate buffer (0.1 M, pH 7.0) was used throughout this research and the corresponding salts were obtained from Merck. ApoHb was prepared from hemoglobin by the HCl–butanone method of Teal [17].

### Methods

**UV-Visible Spectroscopy.** The UV–vis absorption spectra in the range of 250–500 nm were obtained using Cary spectrophotometer, 100 Bio-model, with jacketed cell holders. Spectral changes of 3 μM Hb, ApoHb and Hemin in the presence and absence of Fe<sub>2</sub>O<sub>3</sub> nanoparticle (0, 3, 6, 12, 18, 24, 30, 36, 42 and 48 μM) were recorded by the UV-Visible absorption. All experiments were run in phosphate buffer (0.1 M) at pH 7.0 in a conventional quartz cell thermostated to maintain the temperature at 20 ± 0.1 °C.



**Scheme 1.** Molecular Structure of Hemin Chloride (Hem)

**Circular Dichroism spectroscopy.** Circular Dichroism (CD) measurements in the far-UV CD region (190–260) were done by an Aviv model 215 Spectropolarimeter (Lakewood, NJ, USA) using 1 cm path length, quartz cuvette of 300 μl capacity. Protein solutions were prepared in the buffer. Protein solutions of 0.25 mg/ml were used to obtain the spectra with and without incubation at different concentrations of Fe<sub>2</sub>O<sub>3</sub> nanoparticle (0, 10, 20, 30, 50 μM) for at least 2 min. All spectra were collected in a triplicate from 190 to 260 nm and a back ground-corrected against buffer blank. The results were expressed as ellipticity (deg cm<sup>2</sup> dmol<sup>-1</sup>) based on a mean amino acid residue weight (MRW) of 112 for Hb having the average molecular weight of 64 kDa. The Molar ellipticity values [θ] were obtained using the relation.

$$[\theta] = (100 \times (\text{MRW}) \times \theta_{\text{obs}}/cl) \quad (1)$$

Where  $\theta_{\text{obs}}$  is the observed ellipticity in degrees at a given wavelength,  $c$  is the protein concentration in mg/ml and  $l$  is the length of the light path in cm. All experiments were carried out at 20, 37 and 42 °C.

**Intrinsic fluorescence.** Intrinsic fluorescence intensity measurements carried out at excitation wavelength (280 nm) by a Hitachi Spectrofluorimeter, MPF-4 model, equipped with a thermostatically controlled cuvette compartment. The widths

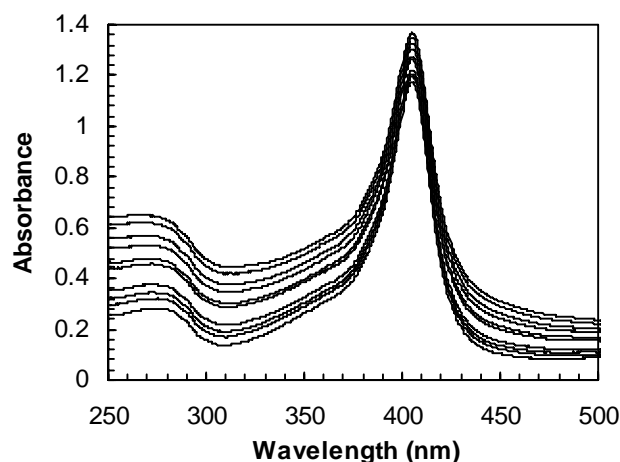


**Fig. 1a.** Absorption spectra of Hb and Fe<sub>2</sub>O<sub>3</sub> nanoparticle–Hb system. Hb concentration was 3 μM and Fe<sub>2</sub>O<sub>3</sub> nanoparticle concentrations from down to up were 0, 3, 6, 12, 18, 24, 30, 36, 42 and 48 μM (T = 20 °C, pH 7.0).

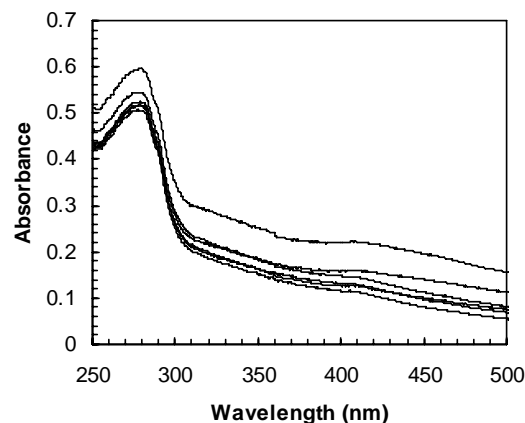


**Fig. 1b.** Absorption spectra of ApoHb and Fe<sub>2</sub>O<sub>3</sub> nanoparticle– ApoHb system. ApoHb concentration was 3 μM and Fe<sub>2</sub>O<sub>3</sub> nanoparticle concentrations from down to up were 0, 6, 12, 18, 30, 42 μM (T = 20 °C, pH 7.0).

of the excitation and the emission slits were set to 10.0 nm and 5.0 nm, respectively. The experiments were repeated in the presence of different concentrations of Fe<sub>2</sub>O<sub>3</sub> nanoparticle (0, 3, 6, 12, 18, 24, 30, 36, 42, 48, 54, 60 and 66 μM). All experiments were carried out at 20, 37 and 42 °C.

## RESULTS AND DISCUSSION

### UV-Visible absorption spectra

Hb has four heme groups located in the crevices (near its surface). There are two absorption peaks (278 and 406 nm) in its UV–vis absorption spectrum. The latter peak, intrinsic absorption peak of Hb, is just the characteristic absorption of the porphyrin–Soret band [18]. UV-vis Soret absorption band of Hb provides the information on the conformational integrity of the heme group region of heme protein [19]. Figure 1a shows the UV–vis absorption spectrum of Hb in the presence of various concentrations of Fe<sub>2</sub>O<sub>3</sub> nanoparticle. The addition of Fe<sub>2</sub>O<sub>3</sub> to the Hb solution leads to a gradual enhancement in the UV peak intensity according to a concentration-dependent relationship. The absorption maximum of Soret band is increased after Fe<sub>2</sub>O<sub>3</sub> nanoparticle treatment, while the maximum absorption wavelengths remain unchanged. The

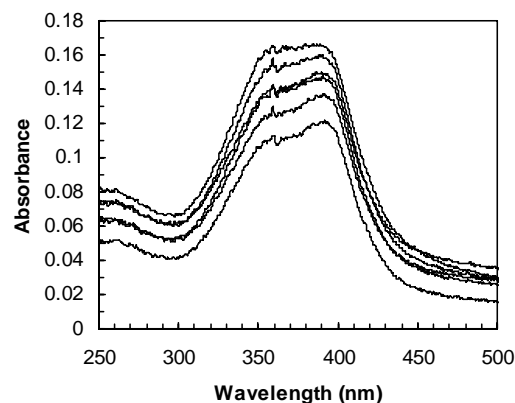


**Fig. 1c.** Absorption spectra of Hemin and Fe<sub>2</sub>O<sub>3</sub> nanoparticle–Hemin system. Hemin concentration was 3 μM and Fe<sub>2</sub>O<sub>3</sub> nanoparticle concentrations from up to down were 0, 6, 12, 18, 30, 42 μM (T = 20 °C, pH 7.0).

increase in UV peak intensity by increasing Fe<sub>2</sub>O<sub>3</sub> nanoparticles may be due to two reasons: (1) Fe<sub>2</sub>O<sub>3</sub> nanoparticles may be inserted predominantly in the native heme orientation, and hence Fe<sub>2</sub>O<sub>3</sub> nanoparticles–hemoglobin formation would be promoted. On the other hand, Fe<sub>2</sub>O<sub>3</sub> nanoparticles can induce the peptide chains in Hb to spread. The amino acids in Hb are exposed gradually. So, by increase

of Fe<sub>2</sub>O<sub>3</sub> nanoparticle concentration, the intensity of the absorption peak increases. Fe<sub>2</sub>O<sub>3</sub> easily integrate into the hydrophobic pocket of Hb due to spreading of peptide chains. The heme groups are released from the hydrophobic cavity of Hb and result in the increase of the intensity of the intrinsic absorption peak. (2) Altering the orientation of heme groups respect to each other in the presence of Fe<sub>2</sub>O<sub>3</sub> nanoparticles. Maybe magnetic field of these nanoparticles can alter orientation of heme groups and the intensity of the long-wavelength transition is increased. The results obtained from UV-visible spectrophotometry provided the further evidence, which confirm the first reason above mentioned. The UV-visible spectra presented in Fig. 1b illustrate the effect of binding of nanoparticles to Apo hemoglobin. These results show that the binding of Fe<sub>2</sub>O<sub>3</sub> nanoparticles cause to spreading the peptide chains in Apo Hb. On the other hand, our results showed that the absorbance of hemin decreased in the presence of Fe<sub>2</sub>O<sub>3</sub> nanoparticle while there is no change in its absorptive wavelength (see Fig. 1c). It illustrated the existence of an interaction between Fe<sub>2</sub>O<sub>3</sub> nanoparticle and hemin. The Soret absorbance reduced in the presence of Fe<sub>2</sub>O<sub>3</sub> nanoparticle, which may be due to the presence of carboxy groups in hemin, which are able to bind to Fe<sub>2</sub>O<sub>3</sub> surfaces.

### Binding property and Fluorescence quenching mechanism of the Fe<sub>2</sub>O<sub>3</sub> nanoparticle to the Hb

The intrinsic fluorescence of proteins containing tryptophan and tyrosine has been used as an important probe in understanding the dynamics and conformational characteristics of these biological macromolecules [16, 20]. Hb contains three Trp residues in each  $\alpha$   $\beta$  dimer, for a total of six in the tetramer: two  $\alpha$ -14 Trp, two  $\beta$ -15 Trp, and  $\beta$ -37 Trp. The intrinsic fluorescence of Hb primarily originates from  $\beta$ -37 Trp.  $\beta$ -37 Trp residue is the nearest in the hemoglobin to the heme. A valuable feature of intrinsic fluorescence of protein is the high sensitivity of tryptophan to its local environment. Changes in emission spectra of tryptophan are common in response to protein conformational transitions, subunit association, substrate binding, or denaturation [21-23].

The effect of Fe<sub>2</sub>O<sub>3</sub> on Hb fluorescence intensity is shown in Fig. 2. Figures 2a, b and c show that the fluorescence intensity of Hb decreases regularly with the increasing

Concentration of Fe<sub>2</sub>O<sub>3</sub> nanoparticle and a quenching of tryptophan fluorescence of Hb at different concentrations of Fe<sub>2</sub>O<sub>3</sub> nanoparticle at 20, 37 and 42 °C, respectively. Tryptophans of Hb are quenched significantly, revealing their interaction with Fe<sub>2</sub>O<sub>3</sub> nanoparticle. There are two kinds of fluorescence quenching, i.e. static quenching and dynamic quenching. For dynamic quenching, the interaction would increase the effective collision number, enhance the energy transfer and increase the quenching constant of the fluorescence substance with increasing the temperature. For static quenching, the stability of the formed compound and the quenching constant would decrease with increasing the temperature [14, 24].

The fluorescence quenching can be described by the well known Stern–Volmer Eq. (2)

$$\frac{F_0}{F} = K_{SV}[Q] + 1 \quad (2)$$

Where  $F_0$  and  $F$  are the steady-state fluorescence intensities in the absence and presence of quencher, respectively,  $K_{SV}$  is the Stern–Volmer quenching constant and  $[Q]$  is the concentration of quencher. The values of  $K_{SV}$  at different temperatures have been summerized in Table 1. The linearity of the  $F_0/F$  versus  $[Q]$  plots is shown in Fig. 3. As given in Table 1, the quenching constant  $K_{SV}$  increases with increasing temperature, which indicates that the probable quenching mechanism of Hb is a dynamic quenching procedure and complex between Fe<sub>2</sub>O<sub>3</sub> nanoparticle and Hb may be formed.

The decrease in maximum intensity by increasing Fe<sub>2</sub>O<sub>3</sub> nanoparticles may be attributed to two factors: (1) The decrease may be due to increase of energy transfer from the  $\beta$ -37 Trp to the neighboring heme group; and (2) Probably, Hb undergo partially unfolded by treatment of nanoparticle. In the native folded state, trp and try are generally located within the core of the protein, whereas in a partially unfolded or unfolded state, they become exposed to the solvent. In a hydrophobic environment (buried within the core of the protein), Tyr and Trp have a high quantum yield and therefore a high fluorescence intensity. In contrast in a hydrophilic environment (exposed to solvent) their quantum yield decreases leading to low fluorescence intensity. However, the first reason was precluded by further investigation as follows: the decrease in maximum intensity of apohemoglobin by

A Spectroscopic Study on the Interaction between Ferric Oxide Nanoparticles

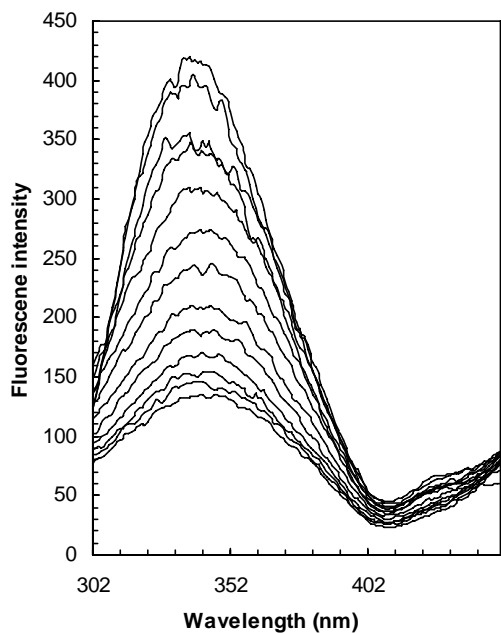


**Fig. 2a.** Effect of 0, 3, 6, 12, 18, 24, 30, 36, 42, 48, 54, 60 and 66 μM Fe<sub>2</sub>O<sub>3</sub> nanoparticle (from up to down) on the fluorescence spectrum of Hb at the temperature of 20 °C (pH 7.4).

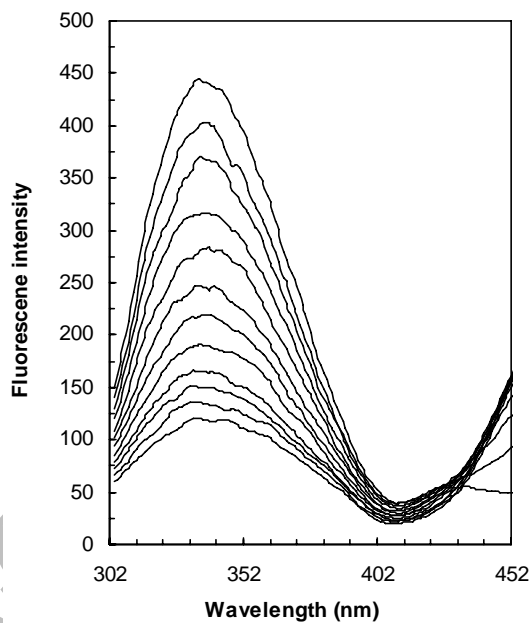


**Fig. 2c.** Effect of 0, 3, 6, 12, 18, 24, 30, 36, 42, 48, 54 and 60 μM Fe<sub>2</sub>O<sub>3</sub> nanoparticle (from up to down) on fluorescence spectrum of Hb at the temperature of 42 °C (pH 7.4).

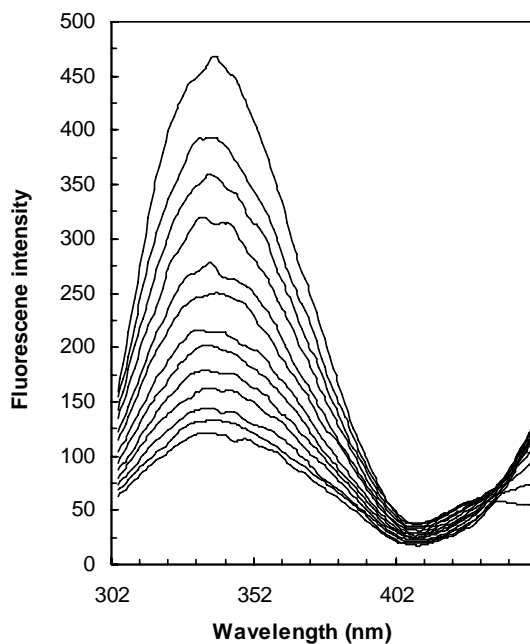


**Fig. 2b.** Effect of 0, 3, 6, 12, 18, 24, 30, 36, 42, 48, 54, 60 and 66 μM Fe<sub>2</sub>O<sub>3</sub> nanoparticle (from up to down) on fluorescence spectrum of Hb at the temperature of 37 °C (pH 7.4).

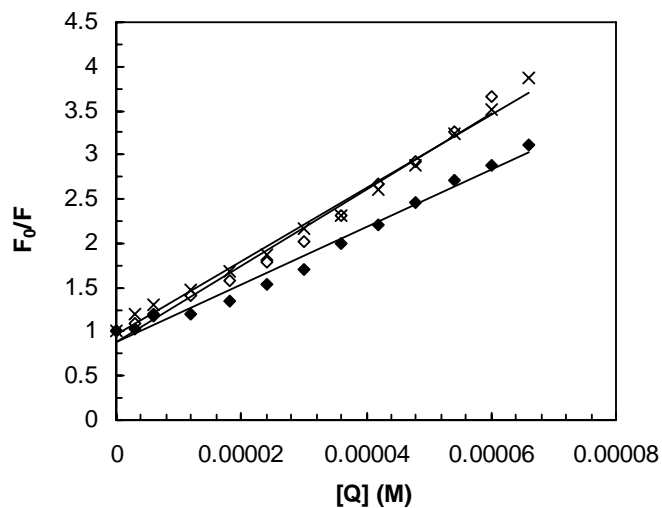


**Fig. 3.** Stern–Volmer plot for the binding of Fe<sub>2</sub>O<sub>3</sub> nanoparticle with Hb at 20 (♦), 37 (×) and 42 °C (◇), respectively.

increasing Fe<sub>2</sub>O<sub>3</sub> nanoparticles were obtained (Fig. 4), which showed that fluorescence quenching is not likely due to energy transfer from the  $\beta$ -37 Trp to the neighboring heme group. On the other hand, the increase in UV peak intensity by increasing Fe<sub>2</sub>O<sub>3</sub> nanoparticles showed that the peptide strands of Hb molecules extended more and amino acids become exposed to the solvent. Accordingly, from UV-vis data and these findings we inferred that Fe<sub>2</sub>O<sub>3</sub> nanoparticles interacted with hemoglobin and caused to form a partially unfolded Hb.

### Binding parameters

The possible number of binding sites (*n*) and binding constant *K* can be determined from the plot of  $\log[(F_0 - F)/F]$  versus  $\log[Q]$  according to the following equation [25, 26] :

$$\log\left[\frac{F_0 - F}{F}\right] = \log K + n \log[Q] \quad (3)$$

A plot of  $\log [(F_0 - F) / F]$  versus  $\log [Q]$  gives a straight line, whose slope equals to *n* and the intercept on Y-axis equals to  $\log K$ . The values of *K* and *n* at 20, 37 and 42 °C have been listed in Table 1 for comparison.

The binding constant and number of binding sites of Fe<sub>2</sub>O<sub>3</sub> nanoparticle decrease by increasing temperature, which indicates decreasing of the affinity of binding Fe<sub>2</sub>O<sub>3</sub> nanoparticle to Hb by increasing temperature. The increasing temperature may be leads unstability of the Fe<sub>2</sub>O<sub>3</sub> nanoparticle-Hb system, therefore this complex is partly decomposed and the values of *K* and *n* decrease [27].

The values of *n* approximately equal to 1 indicate the existence of just a single binding site on Hb for Fe<sub>2</sub>O<sub>3</sub> nanoparticle.

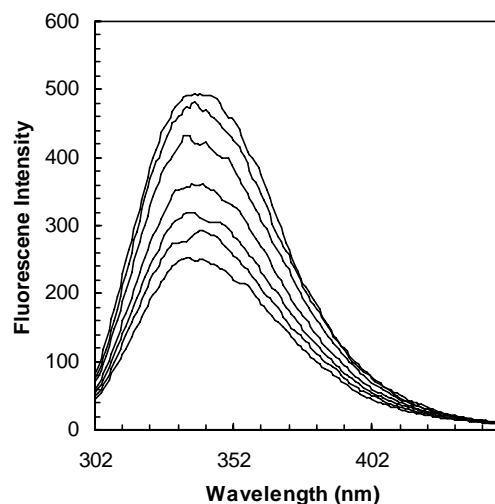


**Fig. 4.** Effect of 0, 6, 18, 30, 48, 60 and 66  $\mu\text{M}$  Fe<sub>2</sub>O<sub>3</sub> nanoparticle (from up to down) on the fluorescence spectrum of ApoHb at the temperature of 20 °C (pH 7.4).

### Thermodynamic parameters and nature of the binding forces

There are four types of noncovalent interactions can play a role in the protein interactions. These are hydrogen bonds, van der Waals forces, electrostatic, and hydrophobic interactions. A quantitative description of the forces that govern molecular associations requires determination of changes of all thermodynamic parameters, including free energy of binding

**Table 1:** Binding parameters and thermodynamic parameters of Hb– Fe<sub>2</sub>O<sub>3</sub> nanoparticle interactions

T (°C)	<i>K</i> <sub>SV</sub> (M <sup>-1</sup> )	<i>K</i> (M <sup>-1</sup> )	<i>n</i>	$\Delta G^\circ$ (kJ/mol)	$\Delta H^\circ$ (kJ/mol)	$T\Delta S^\circ$ (kJ/mol)
20	32683	610942	1.3	-32.9	-115.34	-82.5
37	41406	76736	1.1	-29.5		-85.8
42	43156	54325	1.04	-28.2		-87.2

( $\Delta G^\circ$ ), enthalpy ( $\Delta H^\circ$ ), and entropy ( $\Delta S^\circ$ ) of binding. If the enthalpy change ( $\Delta H^\circ$ ) does not vary significantly over the studied temperature range, then its value and that of  $\Delta S^\circ$  can be determined from the Van't Hoff equation [28]:

$$\ln K = -\frac{\Delta H^\circ}{RT} + \frac{\Delta S^\circ}{R} \quad (4)$$

Where  $K$  is the binding constant at the corresponding temperature and  $R$  is the gas constant. The  $\Delta H^\circ$  and  $\Delta S^\circ$  are determined from the linear van't Hoff plots (Fig. 5). The Gibbs free energy ( $\Delta G^\circ$ ) is estimated from the following equation:

$$\Delta G^\circ = \Delta H^\circ - T\Delta S^\circ \quad (5)$$

$\Delta G^\circ$  reflects the possibility of reaction;  $\Delta H^\circ$  and  $\Delta S^\circ$  are the main parameters to determine molecular forces contributing to the ligand binding. The calculated thermodynamic parameters have been listed in Table 1. The affinity of binding of  $\text{Fe}_2\text{O}_3$  nanoparticle to Hb is decreased by increasing the temperature (from room temperature to 42 °C), which shows a good consistence with exothermic process of binding. The negative sign for  $\Delta G^\circ$  indicates the spontaneity of the binding of  $\text{Fe}_2\text{O}_3$  nanoparticle to Hb. Both  $\Delta H^\circ$  and  $\Delta S^\circ$  have negative

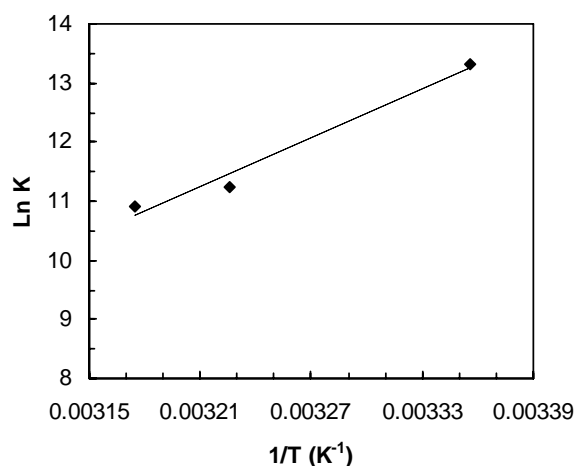


**Fig. 5.** The van't Hoff plot: plot of the natural logarithm of the equilibrium constant versus inverse temperature.

values. The negative values of  $\Delta H^\circ$  and  $\Delta S^\circ$  show that the binding process is an enthalpy-driven and exothermic process. Exothermic and enthalpy-driven binding events are associated with the hydrogen bonding and van der Waals interaction. The functional group on the surface coat (ethylene glycol) of  $\text{Fe}_2\text{O}_3$  is OH, while the main protein functional groups are  $\text{R-COO}^-$  and  $\text{R-NH}_3^+$ . The hydrogen bonding interaction of  $\text{Fe}_2\text{O}_3$ -Hb should occur between the monocoordinated surfaces  $-\text{OH}$  groups and the protonated amine groups in the protein at  $\text{pH} = 7.4$ .

### CD measurements

The CD spectra of Hb exhibited two negative minima at 208 nm and 222 nm, which is typical characterization of the helix structure of class proteins [27]. Figures 6a-c shows the content of helicity of Hb in the presence of different concentrations of  $\text{Fe}_2\text{O}_3$  nanoparticle at 20, 37 and 42 °C.

In the wavelength region of 205–250 nm, the CD spectrum of a protein gives information about its secondary structure. As shown in figure 6a-c the band intensity and positions had not altered, suggesting that binding of  $\text{Fe}_2\text{O}_3$  nanoparticle has not altered the secondary structure of Hb.

In conclusion, if binding of  $\text{Fe}_2\text{O}_3$  nanoparticle induces change in quaternary structure, this should be reflected in the absorption spectrum. However, the absorption spectrum of Hb in the presence of  $\text{Fe}_2\text{O}_3$  nanoparticle (Fig. 1) does not show any major structural change. Also, the CD spectra do not indicate any structural change in Hb induced by the presence of  $\text{Fe}_2\text{O}_3$  nanoparticle (Fig. 6a-c).

### CONCLUSIONS

Our results show that there is a single binding site on Hb for  $\text{Fe}_2\text{O}_3$  nanoparticle. According to thermodynamic parameters, the binding process of  $\text{Fe}_2\text{O}_3$  nanoparticle to Hb is an enthalpy-driven and exothermic process. From UV/vis and fluorescence spectroscopy results, it can be suggested that owing to the binding of  $\text{Fe}_2\text{O}_3$  nanoparticle to Hb, minor conformational changes at the tertiary structure are induced and  $\text{Fe}_2\text{O}_3$  nanoparticle cause to partially unfolding of Hb. The CD spectrum of Hb showed that its secondary structure did not change as well. Taken together, it can be concluded that  $\text{Fe}_2\text{O}_3$

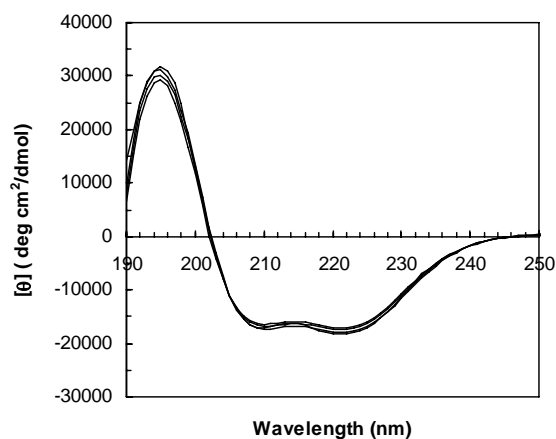


**Fig. 6a.** UV-CD spectra, recorded for Hb and Fe<sub>2</sub>O<sub>3</sub> nanoparticle-Hb system at the Hb concentration of 0.25 mg/ml (T = 20 °C, pH 7.4) and Fe<sub>2</sub>O<sub>3</sub> nanoparticle concentrations (from up to down) of 0, 10, 20 and 40 μM.

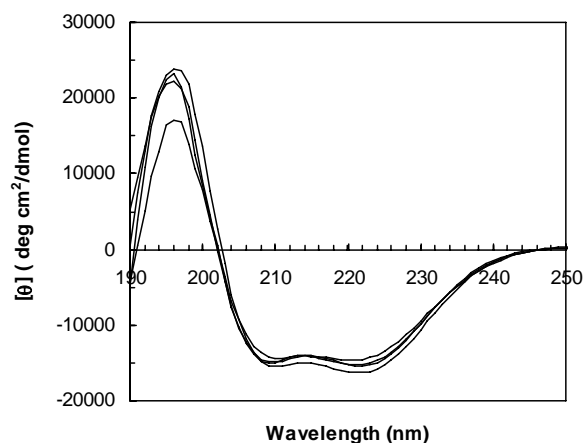


**Fig. 6b.** UV-CD spectra, recorded for Hb and Fe<sub>2</sub>O<sub>3</sub> nanoparticle-Hb system at the Hb concentration of 0.25 mg/ml (T = 37 °C, pH 7.4) and Fe<sub>2</sub>O<sub>3</sub> nanoparticle concentrations (from up to down) of: 0, 10, 20 and 40 μM.

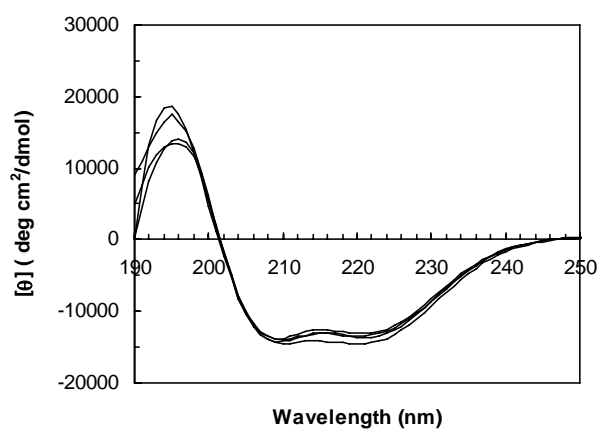


**Fig. 6c.** UV-CD spectra, recorded for Hb and Fe<sub>2</sub>O<sub>3</sub> nanoparticle-Hb system at the Hb concentration of 0.25 mg/ml (T = 42 °C, pH 7.4) and Fe<sub>2</sub>O<sub>3</sub> nanoparticle concentrations (from up to down) of: 0, 10, 20 and 40 μM.

nanoparticle has not a major effects on the hemoglobin structure. Hence, Fe<sub>2</sub>O<sub>3</sub> nanoparticles may inject into the blood for drug delivery and the other applications.

## ACKNOWLEDGEMENTS

The financial support given by the University of Tehran is gratefully acknowledged.

## REFERENCES

- [1] A.S.G. Curtis, C. Wilkinson, Trends Biotechnol. 19 (2001) 97.
- [2] S.M. Moghimi, A.C.H. Hunter, J.C. Murray, Pharm. Rev. 53 (2001) 283.
- [3] J. Panyam, V. Labhasetwar, Adv. Drug. Del. Rev. 55 (2003) 329.
- [4] J.M. Wilkinson, Med. Dev. Technol. 14 (2003) 29.
- [5] D. Sellmyer, R. Skomski, Advanced magnetic nanoparticles, Springer Science, New York, 2006.
- [6] A.S. Arbab, L.A. Bashaw, B.R. Miller, E.K. Jordan, B.K. Lewis, H. Kalish, J.A. Frank, Radio. 229 (2003) 838.



A Spectroscopic Study on the Interaction between Ferric Oxide Nanoparticles

- [7] C.C. Berry, A.S.G. Curtis, *J. Phys. D: Appl. Phys.* 36 (2003)198.
- [8] U. Häfeli, W. Schütt, J. Teller, M. Zborowski, *Scientific and clinical applications of magnetic carriers*, Plenum Press, New York, 1997.
- [9] Q.A. Pankhurst, J. Connolly, S.K. Jones, J. Dobson, *J. Phys.D: Appl. Phys.* 36 (2003)167.
- [10] P. Reimer, R. Weissleder, *Radio*. 36 (1996) 153.
- [11] E.X. Wu, H. Tang, K.K. Wong, J. Wang, *J. Magn. Reson. Imag.* 19 (2004) 50.
- [12] A. K. Gupta, M. Gupta, *Biomaterials* 26 (2005) 3995.
- [13] H.M. Johng, J.S. Yoo, T.J. Yoon, H.S. Shin, B.C. Lee, C. Lee, J.K. Lee, K.S. Soh, *Evid. Based Complement Alternat. Med.* 4 (2007) 77.
- [14] Y.Q. Wanga, H.M. Zhangb, G.C. Zhanga, S.X. Liub, Q.H. Zhou, Z.H. Feia, Z.T. Liua, *Int. J. Biol. Macromol.* 41(2007) 243.
- [15] M.F. Perutz, *Scientific American*, vol. 6, 2005.
- [16] G. Weber, *Adv. Protein Chem.* 8(1953) 415.
- [17] F.W. Teale, *J. Biochim. Biophys. Acta* 35 (1959) 543.
- [18] B. Sengupta, P.K. Sengupta, *Biochem. Biophys. Res. Commun.* 299 (2002) 400.
- [19] W. Sun, D. Wang, Z. Zhai, R. Gao and K. Jiao, *J. Iran. Chem. Soc.* 6 (2009) 412.
- [20] F.W.J. Teale, G. Weber, *Biochem. J.* 72 (1959) 156.
- [21] B. Alpert, D.M. Jameson, G. Weber, *J. Photochem. Photobiol.* 31(1980) 1.
- [22] R.A. Goldbeck, R.M. Esquerra, D.S. Kliger, *J. Americ. Chem. Soc.* 124 (2002) 7646.
- [23] S. Venkateshrao, P.T. Manoharan, *Spectrochim. Acta Part A* 60 (2004) 2523.
- [24] J. Zhoua, X. Wua, X. Gua, L. Zhou, K. Songa, S. Weia, Y. Fenga, J. Shena, *Spectroc. Acta Pt. A-Molec. Biomolec. Spectr.* 72 (2009) 151.
- [25] M. Jiang, M.X. Xie, D. Zheng, Y. Liu, X.Y. Li, X. Chen, *J. Mol. Struct.* 692 (2004) 70.
- [26] J.Q. Lu, F. Jin, T.Q. Sun, X.W. Zhou, *Int. J. Biol. Macromol.* 40 (2007) 299.
- [27] Y.J. Hu, Y. Liu, X.S. Shen, X.Y. Fang, S.S. Qu, *J. Mol. Struct.* 738 (2005) 143.
- [28] P. Atkins, J. De Paula, *Physical Chemistry*, 8<sup>th</sup> Ed., W.H. Freeman and Company, 2006, pp. 212-220.

Archive of SID.ir